Influence of nodule count, austenitising variables and matrix on ductile iron decarburisation

A. D. Sosa[1,2], O. J. Moncada[1,2] and J. Sikora*[2]

The surface decarburisation produced during the austenitising stage of ductile iron parts constitutes an issue that needs to be addressed in many manufacturing processes. This work examines the role that nodule count and other variables play on decarburisation onset and decarburised layer thickness. Specimens with noticeable different nodule counts were employed to perform the experiments. The results showed that the thickness of the decarburised layer markedly decreases as nodule count increases, and that the decarburised layer depth increases as the austenitising holding time increases. On the other hand, the austenitising temperature has little influence on the decarburisation process. An equation able to calculate the decarburisation onset, the austenitising holding time and the decarburised layer thickness was developed. This equation yields accurate estimations for austenitising ductile iron parts with prior ferritic matrixes, and is further applicable to a wide range of nodule counts, which even comprise those proper of thin wall ductile iron parts.

Keywords: Ductile iron, Nodule count, Decarburising, Austenitising holding time

Introduction

The engineering community is strongly pressed to produce lighter, stronger and stiffer metallic parts. Ductile iron (DI) can be a material of choice to fabricate numerous parts, since it is suitable to produce highly resistant cast parts of complex shape; besides, it is relatively inexpensive.

To make full use of the relative advantages of manufacturing light parts, DI is being cast with thin walls. Reducing DI thickness allows designing and casting hollow parts of high stiffness. Nevertheless, as parts thickness diminishes, the metallurgical quality of thin wall ductile iron (TWDI) parts becomes increasingly compromised and less amount of material can be removed by machining. Casting defects and microstructural anomalies, such as microshrinkage, free carbides, defective microconstituents and decarburised areas, can significantly decrease mechanical properties.

A vast range of mechanical properties can be obtained from DI through heat treatments, enhancing the strength/weight and strength/cost ratios. Most heat treatment cycles enable an austenitising stage. If no adequate protective atmosphere is employed, surface alterations, such as corrosion and decarburisation, could arise. In particular, the decarburisation of the metallic matrix is an operative problem faced by many manufacturing processes wherein high temperatures are involved, since carbon is a key element in the chemical composition of DI parts with highly resistant matrixes (i.e. martensitic, bainitic, ausferritic and pearlitic). As temperature rises, carbon atoms increase their mobility to a greater extent than the other elements comprising the alloy, making them possible to migrate to the surface and to combine with the oxygen of the atmosphere, forming CO_2.

The presence of decarburised areas (ferritic zones) can affect hardness and wear resistance. Moreover, a small decarburised area can locally diminish yield and rupture stress by modifying the microstructure, thereby resulting in a weaker area. This can get plastically deformed and turn into a stress concentrator, seriously affecting fatigue resistance.[1] The ISO 3887 standard establishes two methods for decarburisation control, direct optical observation and microhardness profiles. Mercier *et al.*[2] concluded that metallographic observations underestimate decarburisation depth, thereby recommending the use of microhardness profiles. As for the industrial practice, on the other hand, hardness tests constitute a practical control method when it comes to determining the effectiveness of heat treatments.

The problem posed by decarburisation can be avoided using protective atmospheres during heat treatment, or even solved if the parts surface is machined afterwards.

Notwithstanding this, the latter does not always apply if the decarburised surface areas cannot be removed by

[1]Mechanical Technology Research Group, UNMDP, Juan B. Justo 4302, (B7608 FDQ) Mar del Plata, Argentina
[2]Metallurgy Division INTEMA (UNMDP) – CONICET, RA-7600 Mar Del Plata, Buenos Aires, Argentina

*Corresponding author, email jsikora@fi.mdp.edu.ar

Received 16 August 2008; accepted 4 February 2010
DOI 10.1179/136404610X12693537270055

International Journal of Cast Metals Research ijc932.3d 13/4/10 14:07:21
The Charlesworth Group, Wakefield +44(0)1924 369598 - Rev 7.51n/W (Jan 20 2003)

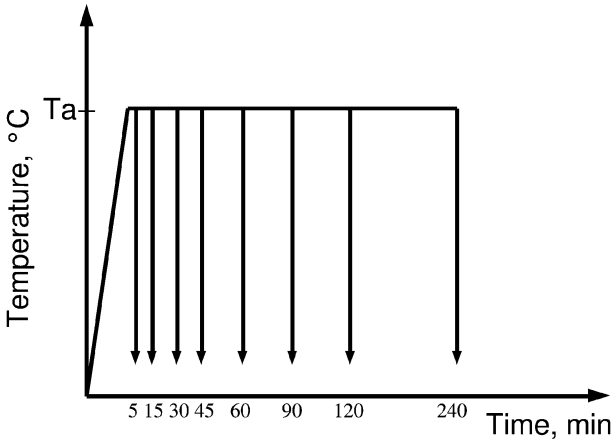

1 Schematic representation of decarburising heat treatment cycles

machining and are subjected to high stress in service. This could be the case of complex shaped parts, or of inner surface regions of hollow, highly resistant parts, to name a few.

On the other hand, DI parts can exhibit a wide range of nodule counts as a result of the inoculation process, and principally of the cooling rate imposed during solidification; in particular, TWDI parts can increase the nodule count in about one order of magnitude when compared with thicker parts.[3–6] Some researchers, who explored the kinetics of solid state transformations on DI of varied thicknesses, have found that solid state transformations involving carbon transport from the matrix to the nodules or *vice versa*, such as austenitising or ferritising, show faster kinetics as the nodule count increases.[7,8]

This work studies the surface decarburisation produced during the austenitising step of DI parts of diverse thickness, and aims at evaluating the influence of nodule count and austenitising holding time, among other variables.

Experimental procedure

An unalloyed DI melt was prepared in a medium frequency induction furnace. Steel scrap and foundry returns were used as raw materials. The melt was heated up to 1540°C before pouring. Nodulisation was carried out using the sandwich method adding 1·5 wt-%Fe–Si–Mg (6 wt-%Mg). The melt was inoculated with 0·6 wt-%Fe–Si (75 wt-%Si) in a separate ladle. A Baird DV6 spectrometer was used to determine the chemical composition of the melt.

Thin plates of 2 and 4 mm thicknesses and 'Y' blocks of 12·5 and 25 mm (ASTM A395) were cast in sand moulds in order to obtain four noticeably different nodule counts as a consequence of markedly different cooling rates imposed by the parts thicknesses. The moulds were made using AFS-60 silica sand and alkyd resin as a binder.

Table 1 Decarburising heat treatment conditions

T_a, °C	Austenitising time t, min							
870	…	…	…	45	…	90	…	…
900	5	15	30	45	60	90	120	240
930	…	…	…	45	…	90	…	…

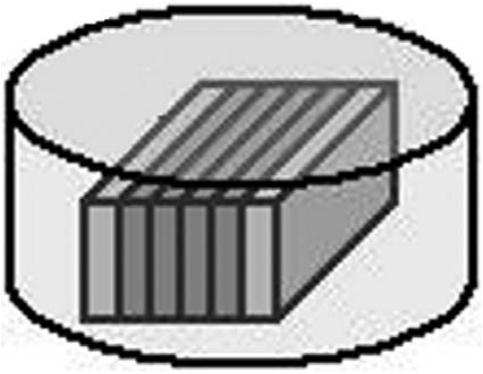

2 Layout of metallographic samples 3

Prismatic samples were premachined from the 'Y' blocks and plates. All of them presented matrixes composed of different percentages of pearlite and ferrite in the as cast condition. They were ferritised by annealing at 900°C for 3 h in an electric furnace, and followed by a slow cooling stage. This heat treatment allowed obtaining entire ferritic matrixes (no carbon in the matrix). Additionally, one batch containing samples of all nodule counts was pearlitised in order to obtain a set of specimens with pearlitic matrixes (carbon in the matrix).

Final specimens were then machined from all the samples. They were cut and squared off to dimensions of $13 \times 12{\cdot}5$ mm under low energy cutting conditions, and afterwards, they were recessed by mechanical shaping until reaching 1·5 mm in thickness. Then, the specimens were manually polished with SiC up to grit 600 before being submitted to heat treatment. Each specimen had a hole of 2·5 mm in diameter near the corner to enable their holding and manipulation during heat treatment.

Several sets of specimens were prepared. Each set included four specimens (one specimen from each nodule count). All sets were placed equidistantly on a wiring frame; face up and in contact with the furnace atmosphere. This arrangement enables not only to load several specimens at the same time, but also to remove one set at a time, leaving the rest in the furnace to complete their heat treatment.

Decarburising heat treatments were carried out by introducing all sets of specimens into a furnace preheated at a specific austenitising temperature $T = T_a$ (°C). The sets were removed from the furnace after holding for periods ranging from 5 to 240 min. Then, the specimens were water quenched and afterwards washed, dried and marked. Figure 1 shows a schematic diagram of the decarburising heat treatments, while Table 1 summarises the temperatures T_a and holding times t corresponding to all the sets used in this work.

The thicknesses of the decarburised layers were determined by digital images analysis. To do so, transversal cuts were made on the specimens. Then the specimens of each batch were mounted with their faces aligned at 90° angle to the observation plane (Fig. 2), and finally polished and etched with nital (2%) to carry out metallographic observations.

For each specimen, optical micrographies of different magnifications were taken and five measurements of the decarburised thickness were made on each of them. The maximum thickness and decarburised layers' averages were calculated for each specimen. The decarburised

International Journal of Cast Metals Research ijc932.3d 13/4/10 14:07:21
The Charlesworth Group, Wakefield +44(0)1924 369598 - Rev 7.51n/W (Jan 20 2003)

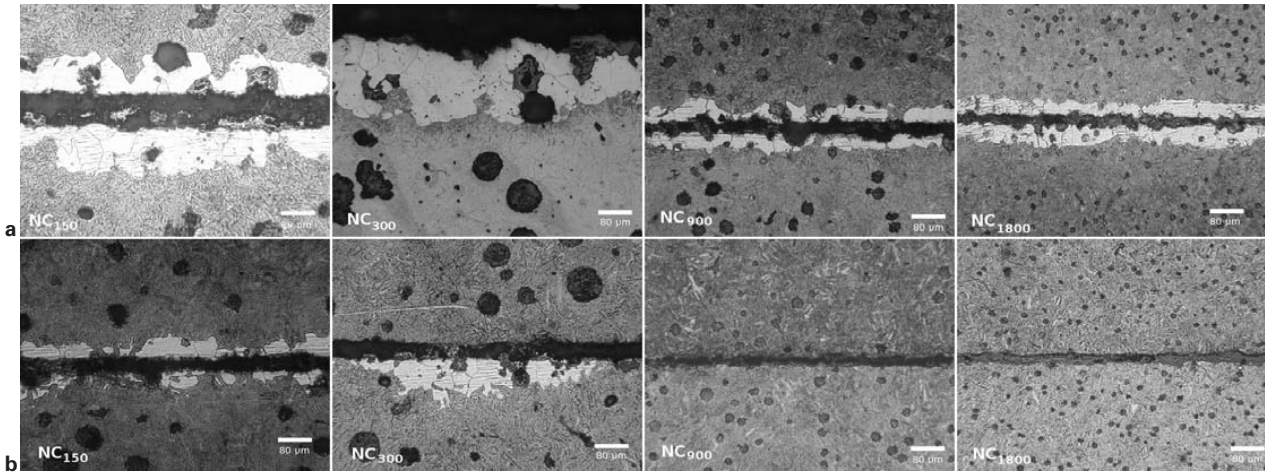

a austenitised for 45 min; *b* austenitised for 15 min

3 Cross-sectional structure of heat treated samples for all nodule counts (etched with 2% nital)

thickness of ferritic zones whose areas were smaller than those of the largest nodules present in the analysed zone, was considered null.

Microhardness profiles were obtained according to ISO 3887 standard. Micro Vickers indentations were performed every 5 μm from the surface up to 150 μm beneath using a 0·15 N load.

Results and discussion

The final chemical composition (wt-%) of the melt was as follows: C=3·53, Si=2·98, Mn=0·14, S=0·013, P=0·03, Mg=0·045, Ce=0·016, Cr=0·04, Cu=0·07, Ni=0·04, Mo and Ti<0·01. The carbon equivalent (CE) was slightly hypereutectic: CE=C+(Si+P)/3=4·52.

Table 2 summarises the average nodule count, sphericity and nodularity (ASTM A247) for the specimens of all thicknesses.

Figure 3 depicts cross-sectional micrographies corresponding to the specimens of all nodule counts under study, austenitised at 900°C for different periods of time. The decarburised areas are revealed as clear areas of ferrite near the specimen surface, while the grey areas relate to martensitic structure. Black bands are bakelite.

Influence of nodule count and austempering time

All the specimens austenitised for more than 45 min exhibited surface decarburisation. Figure 3*a* shows that the thickness of the decarburised layers is nearly uniform. Regarding the shortest austenitising holding times (5 and 15 min), the decarburised areas evidenced in the NC_{150} and NC_{300} specimens were slightly higher than those of the nodules in contact with the surface (Fig. 3*b*). No decarburisation was detected in the specimens with high nodule count (NC_{900} and NC_{1800}) austenitised for less than 30 min.

Table 3 lists the average values and the variation ranges of the decarburised layer thickness for all the conditions tested.

Figure 4*a* shows the maximum decarburised thickness values as a function of the austenitising holding time t for the specimens with different nodule counts. As observed, the depth of the decarburised layer increases with increasing holding time. In addition, NC_{150} and NC_{300} specimens feature an earlier decarburisation onset if compared toNC_{900} and NC_{1800} respectively. When austenitising holding time increases, a similar evolution of the decarburised thickness can be appreciated for all the specimens.

Figure 4*b* depicts the different depths of the decarburised layer as a function of the nodule count for each austenitising time t. It can be clearly observed that the thickness of the decarburised layer decreases as nodule count increases for all the holding times analysed. For instance, considering NC_{150} and NC_{300} specimens austenitised for 60 min (time lapse of common choice in the industrial practice for parts of up to 25 mm in thickness), the decarburised layer thickness is seen to nearly double those observed in NC_{900} and NC_{1800} specimens. On the other hand, only specimens with low nodule count (NC_{150} and NC_{300}) showed decarburisation for holding times of less than 30 min.

Depth variations in the decarburised layer can be associated with carbon diffusion path modifications, which may occur when the nodule count increases, i.e.

(i) the diffusion distance decreases (shorter inter-nodular distances)
(ii) the amount of nodule/matrix interfaces rises

Table 2 Microestructural characteristics of specimens

Thickness mm	Nodule count*, nod/mm^2	Nodularity, %	Sphericity	Specimen identification
2	1800	90	0·9	NC_{1800}
4	900	90	0·86	NC_{900}
12·5	300	80	0·85	NC_{300}
25	150	80	0·81	NC_{150}

*The minimum diameters for considering a graphite particle as a nodule were 5 μm for samples containing 900 and 1800 nods/mm and 10 μm for samples containing 150 and 300 nods/mm^2.

International Journal of Cast Metals Research ijc932.3d 13/4/10 14:07:23
The Charlesworth Group, Wakefield +44(0)1924 369598 - Rev 7.51n/W (Jan 20 2003)

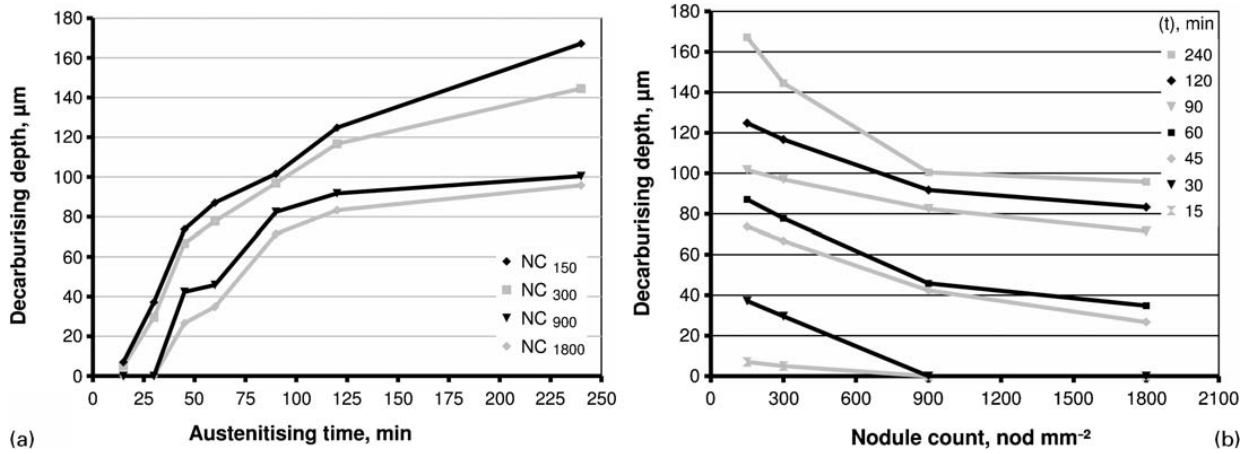

4 Maximum decarburised depth on samples austenitised at 900°C as function of *a* holding time and *b* nodule count

(iii) the number of preferential diffusion paths increases (greater number of grain boundaries).

Grain boundary diffusion is much quicker than bulk diffusion, yet the total diffusion contribution is not that large, as the area in which it takes place is minimal. To achieve a pronounced difference, there should be a great number of grain boundaries.[9] The metallographic studies conducted on different specimens showed that the variation in grain size turned out to be slightly significant. In fact, grain size variation ranged from 7 to 8, according to ASTM E112-96, among the specimens obtained from the 25 mm 'Y' blocks and the 2 mm plates. Nodule count variation, in turn, was of one order of magnitude, and so the effect of grain size was disregarded. Nodule count variation significantly affects the other two factors mentioned above by modifying the internodular distances and the amount of nodule/matrix interfaces to a large extent. As a consequence, if the total volume of graphite is considered to be the same in all the specimens (they were all made from the same melt and their matrix were fully ferritic) and the morphologies of all free graphite are considered to be spherical, the following relationships between volumes V and areas S could be established

$$V_1 = V_2 = V_i = \mathrm{NC}_i \frac{4}{3}\pi r_i^3 \tag{1}$$

$$S_i = \mathrm{NC}_i 4\pi r_i^2 \tag{2}$$

where NC is the volume of nodule count calculated as $\mathrm{NC}_i = (\mathrm{NC}_{surface})^{3/2}$ for a simple cubic packing and r is the average ratio of the nodules. From equations (1) and (2), the following can be obtained

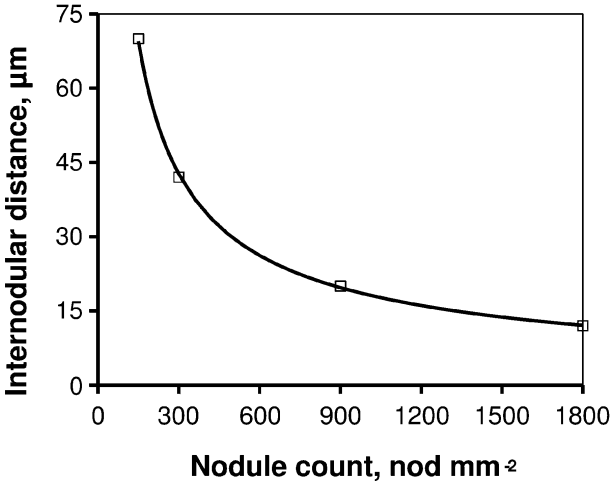

5 Average internodular distance

$$r_1 = r_2 \left(\frac{\mathrm{NC}_2}{\mathrm{NC}_1}\right)^{1/3} \tag{3}$$

$$\frac{1}{4\pi} = \frac{r_2^2 \mathrm{NC}_2}{S_2} = \frac{r_2^2}{S_1}\left(\frac{\mathrm{NC}_2}{\mathrm{NC}_1}\right)^{2/3} \mathrm{NC}_1 \tag{4}$$

Then, it is possible to obtain the equation as below

$$S_{1800} = S_{150}\left(\frac{\mathrm{NC}_{150}}{\mathrm{NC}_{1800}}\right)^{-1/3} \tag{5}$$

This relationship allows determining that $S_{1800} = 3{\cdot}464 S_{150}$, which means that the amount of nodule/matrix interfaces increases more than three times when the nodule count goes from 150 to 1800 nods/mm. A

Table 3 Average decarburisation depth and variation ranges, μm

T_a, °C	870		900							930	
t, s	45	90	5	15	30	45	60	90	120	240	45	90
Sample												
NC_{150}	70±2·6	91±4·2	0	3·5±3·5	34·6±2·5	71·2±2·5	83·7±3·3	95·8±5·8	117·3±7·5	156·2±11	72·5±3·5	113·4±5·6
NC_{300}	64·6±1·2	90·5±2·9	0	2·5±2·5	28·6±1	65±1·5	73·2±4·6	90·9±6	108·5±8·1	132·5±12	66·4±3·2	104·2±4·9
NC_{900}	39·4±0·6	67±2·7	0	0	0	40±2·3	43·3±2·5	76·2±6·2	85·7±6	92·8±7·6	49,2±3	84·3±3·3
NC_{1800}	25·4±0·7	69·4±2	0	0	0	25·7±1	32,8±2	69·5±1·9	67·2±4·2	76±7·3	30·5±2	75·9±2·4

International Journal of Cast Metals Research ijc932.3d 13/4/10 14:07:25
The Charlesworth Group, Wakefield +44(0)1924 369598 - Rev 7.51n/W (Jan 20 2003)

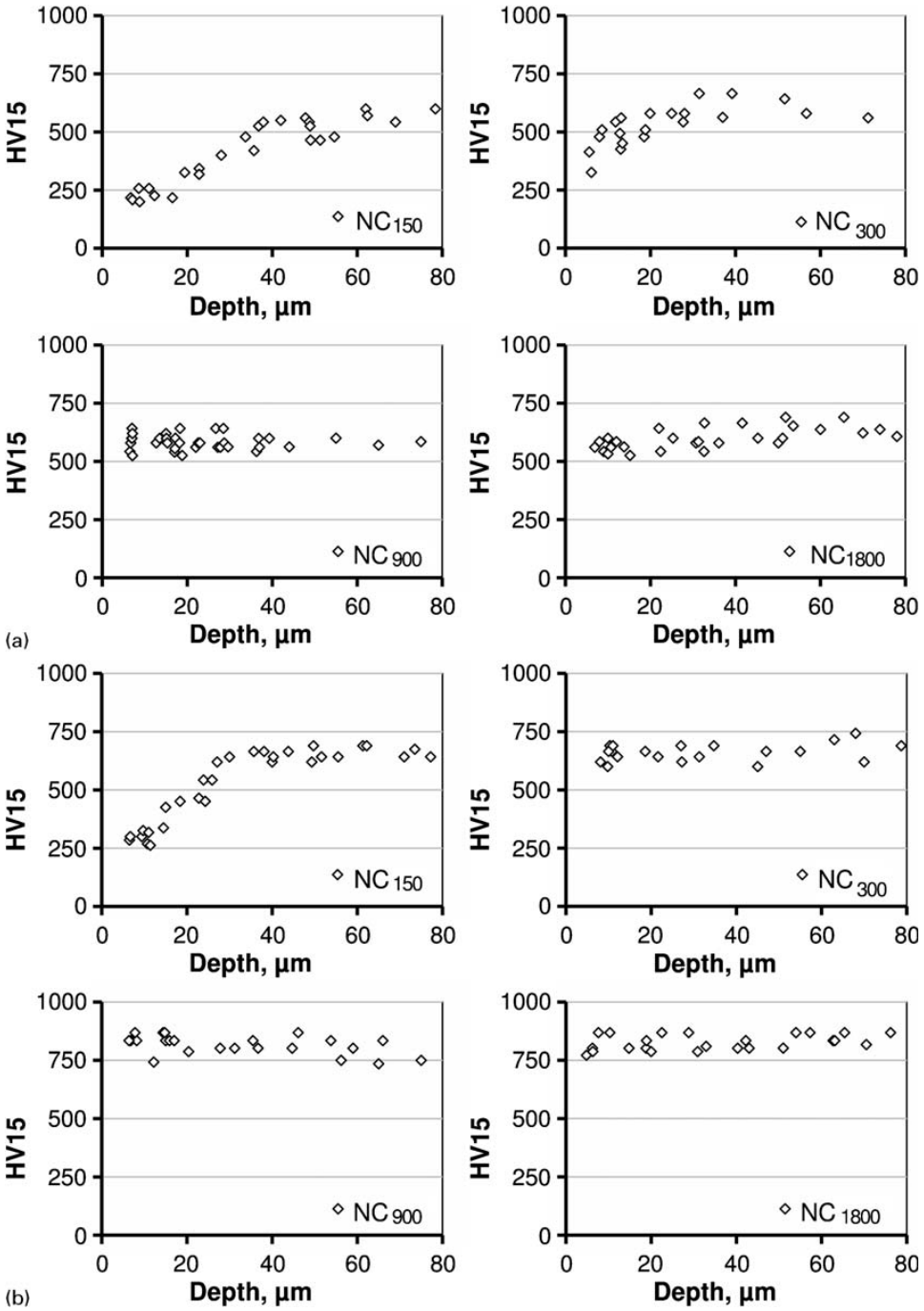

6 Microhardness profiles (HV_{15}) of specimens austenitised for *a* 5 min and *b* 15 min

similar result could be obtained using other models. It has also been checked that if the lack of sphericity (table 2) is considered regarding the increase in the nodule area, no significant changes are produced.

On the other hand, Fig. 5 illustrates the way in which the average distance between nodules surfaces varies as a function of nodule count. These paths were obtained by direct measurements performed on samples. The metallographic studies allowed establishing that the 'longest way' that carbon atoms need to travel from a nodule to the farthest away possible place in the matrix (considering bulk carbon diffusion) amounts to 0·5–0·7 times the average distance value, depending on whether a local configuration of four (hcp or fcc lattice type) or five (bcc lattice type) neighbouring nodules surrounding each nodule is adopted. Therefore, if all the other variables affecting diffusion are considered constant, it is possible to state that carbon saturation in the matrix occurs more quickly as the nodule count increases.

As regards entirely ferritic matrix, it can be assumed that no carbon loss occurs during the first austenitising stage as matrix carburisation would occur first. At this stage, carbon atoms travel from the nodules to the matrix which, in turn, gradually transforms into austenite. Nonetheless, as matrix carburisation is partially or totally reached, the carbon atoms located near the surface are able to combine rapidly with the atmospheric oxygen, leaving the metallic matrix and getting lost. If carbon provision from the nodules is insufficient to compensate such a loss, an inverse concentration gradient of carbon is created in the areas near the surface, wherein the effective decarburisation of

International Journal of Cast Metals Research ijc932.3d 13/4/10 14:07:32
The Charlesworth Group, Wakefield +44(0)1924 369598 - Rev 7.51n/W (Jan 20 2003)

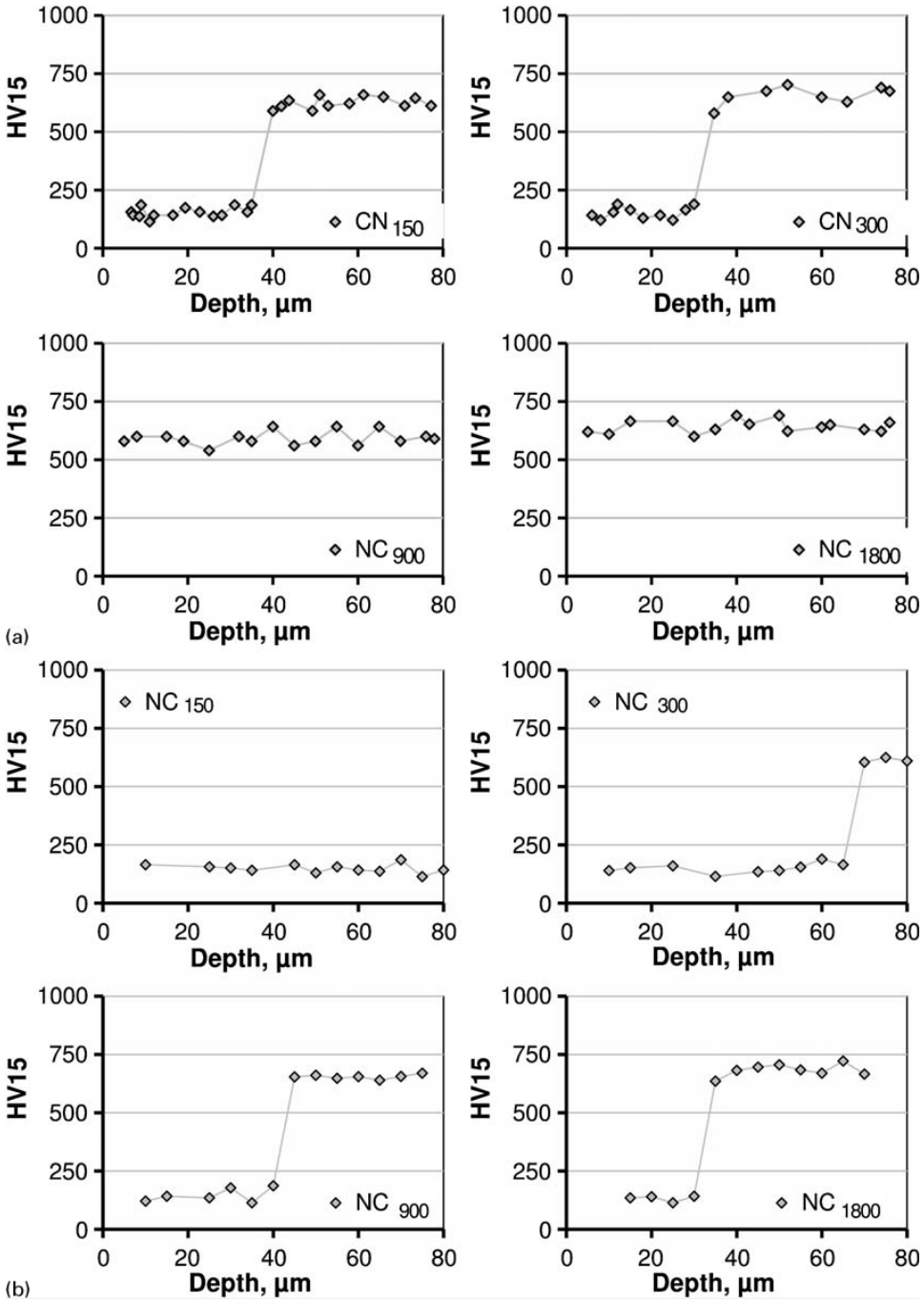

7 Microhardness profiles (HV_{15}) of specimens austenitised for *a* 30 min and *b* 60 min

the material takes place. Taking the preceding into account, the shorter the diffusion distance (when nodule count increases), the more effective the nodule carbon provision.

Microhardness profiles

Figure 6 illustrates microhardness profiles from cross-sectioned specimens austenitised at 900°C for 5 and 15 min respectively. In general, an increase in hardness with time and a gradient in the surface area of NC_{150} and NC_{300} specimens are noticed. This allows confirming that the carburisation of the metallic matrix during the first austenitising stage is more efficient in NC_{900} and NC_{1800} specimens. Moreover, the matrix microhardness values correspond to those expected for low carbon martensite (>250 HV), thereby indicating that carburisation has occurred before ferritic zone starts growing.

Figure 7 shows microhardness profiles of cross-sectioned specimens austenitised for 30 and 60 min respectively. NC_{900} and NC_{1800} specimens treated for 30 min yielded no significant hardness variations along the profile. NC_{150} and NC_{300} specimens, on the contrary, yielded very low hardness in the surface and increased significantly as depth did. In this respect, all the specimens austenitised for 60 min behaved in a similar manner, demonstrating that the abrupt variation in hardness occurs nearer the surface as nodule count increases. Metallographic observations evidenced that this variation is directly associated to the ferritic–martensitic microstructure change, since for all the cases analysed, the correlation of the decarburised layer

International Journal of Cast Metals Research ijc932.3d 13/4/10 14:07:43
The Charlesworth Group, Wakefield +44(0)1924 369598 - Rev 7.51n/W (Jan 20 2003)

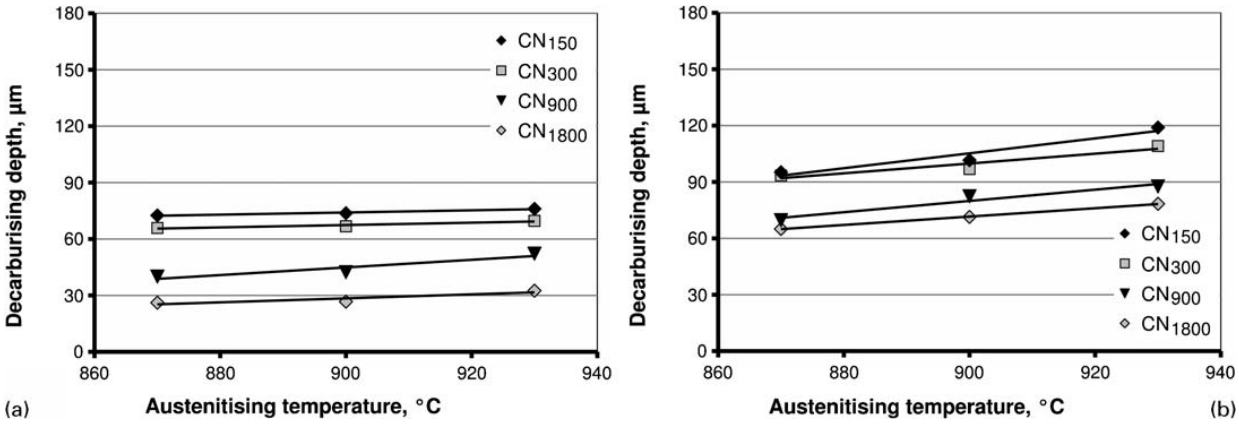

8 Maximum decarburised depth on samples austenitised at different temperatures for holding times of *a* 45 min and *b* 90 min

thickness data obtained by both methods turned out to be very good.

Influence of temperature on decarburisation

Figure 8 shows the decarburisation thickness obtained during austenitising treatments at different temperatures for holding times of 45 and 90 min respectively. Within the range analysed, temperature plays an insignificant role compared with that adopted by nodule count and holding time, and therefore, it is not considered a meaningful variable.

Quantitative prediction of decarburisation

An empiric equation was developed to predict decarburisation onset and decarburised thickness for austenitising treatments at $\sim$900°C. Even though each real problem requires a complex treatment of its own, given the great number of variables that may be involved in the process, they have been delimited to favour mathematical calculation. Therefore, focus was set on finding expressions enabling to calculate decarburisation as a function of nodule count and austenitising time in specimens with prior ferritic matrixes.

Making use of first Fick's law, the following simplified relationship to relate the diffusion distance x, time t and diffusion coefficient D (which, in turn, is a function of temperature T_a) can be established

$$x=(Dt)^{1/2} \tag{6}$$

By sketching the maximum decarburised thickness values as a function of $t^{1/2}$, lineal regressions with very good adjustment can be obtained (Fig. 9). The curves slopes were found to change at longer times (>60 min). This behaviour can be ascribed to the fact that the ferrite surface acts as a diffusion barrier after prolonged holding times turning the decarburising rate smaller. However, to adapt the pattern to time periods of possible industrial interest, the analysis was circumscribed to a maximum of 60 min.

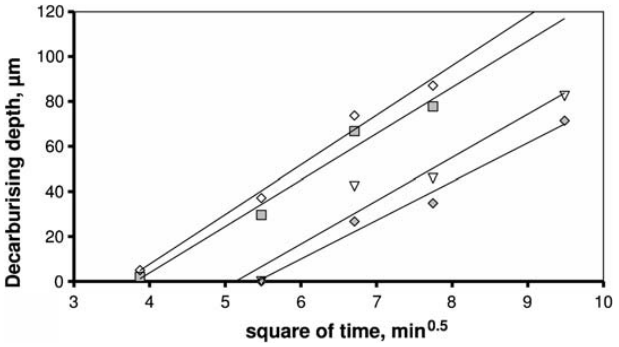

9 Lineal regressions of maximum decarburised thickness on specimens with prior ferritic matrixes austenitised at 900°C

By rotating the axes in Fig. 9, the equation of each straight line can be defined as follows

$$(t)^{1/2}=ad-(t_0) \tag{7}$$

where d is the decarburised thickness, a is a coefficient dependent on nodule count and the ordinate on the origin t_0 is the time of decarburisation onset, also dependent on nodule count.

After reordering the equation to obtain the decarburised thickness, the following expression is obtained

$$d=\frac{(t)^{1/2}}{a}+\frac{(t_0)^{1/2}}{a} \tag{8}$$

By means of the data obtained from the straight lines in Fig. 9, and sketching them as a function of NC (Fig. 10), the following equations can be obtained

$$a=7{\cdot}106\times10^{-6}\mathrm{NC}+4{\cdot}543\times10^{-2} \tag{9}$$

$$t_0=-8{\cdot}59\times10^{-6}\mathrm{NC}^2+0{\cdot}0271\mathrm{NC}+8{\cdot}521 \tag{10}$$

The maximum treatment time in which there is no surface decarburisation for a given nodule count can be easily calculated with equation (10) (Fig. 9). Likewise, knowing NC, equations (9) and (10) can be used to complete equation (8) and thereby predict in an accurate manner the decarburised thickness for a given austenitising holding time. These equations could be used to predict decarburisation in production processes.

Influence of other variables on decarburisation prediction

To consider the influence of the initial microstructure on decarburisation, specimens with pearlitic matrixes (high carbon content in the metallic matrix) were also studied. Figure 11 lists the results derived from NC_{300} and NC_{900} specimens with pearlitic matrix, whose carbon content was close to 0·85 wt-%. In this case, the lineal adjustments made were also good. If Figs. 9 and 11

International Journal of Cast Metals Research ijc932.3d 13/4/10 14:07:55
The Charlesworth Group, Wakefield +44(0)1924 369598 - Rev 7.51n/W (Jan 20 2003)

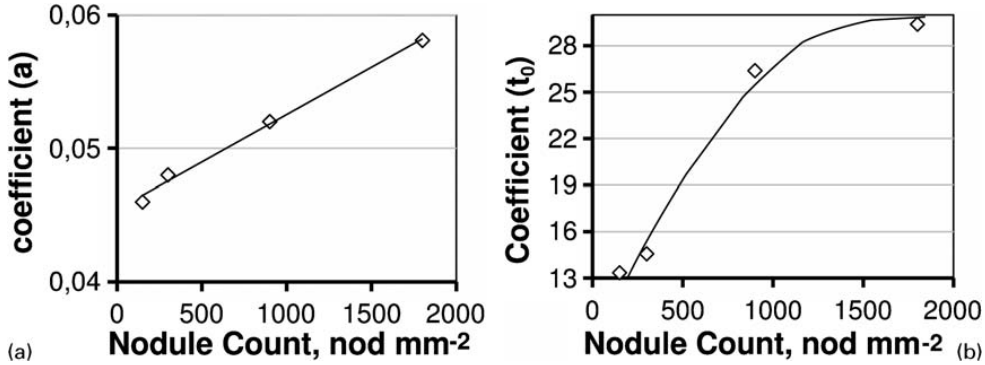

10 Relationships between time t_0, coefficient a and nodule count

are compared, an earlier decarburisation onset can be appreciated in the specimens with pearlitic matrix in comparison to ferritic ones. Such difference could be attributed to the fact that upon austenitisation start, the matrix is already saturated with carbon, and hence, it can immediately begin getting lost. Concurrently, a slower advance of the decarburisation process is observed as a function of time.

To incorporate the effect of the initial carbon content in the matrix, it would be necessary to multiply coefficients a and t_0 in equations (9) and (10) respectively, by the correction factors dependent on the percentage of carburised phases and their carbon content. However, the incorporation of the microstructure effect in the previously formulated equation was not considered convenient, as it was constructed to be applied to austenitisation process of DI with prior ferritic matrixes and principally TWDI parts with high nodule count, austenitised without protective atmospheres. It is important to point out that TWDI parts are usually cast using high Si content to favour graphitisation and avoid carbide formation. This, added to the large number of graphite nodules acting as sinks during the cooling stage in solid state, promotes predominantly as cast ferritic matrixes.

To assess the effect of the austenitising temperature on decarburisation, a type b (T=900°C) term, with b in the range of 0·06–0·10 and in agreement with the nodule count, could be added to equation (8). However, as demonstrated above, the effect of temperature within the studied ranges turned out to be insignificant in comparison with that exerted by nodule count and holding time, and therefore, it was disregarded.

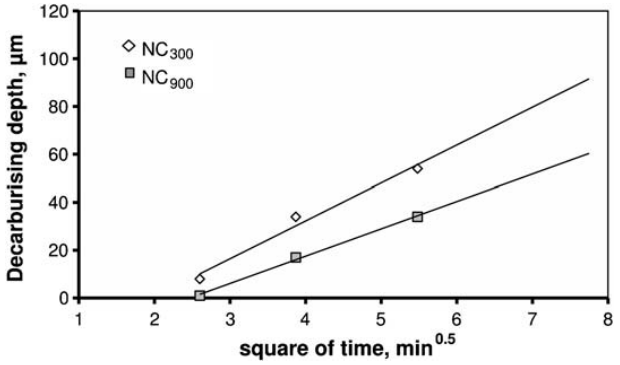

11 Lineal regressions of maximum decarburised thickness on pearlitic specimens austenitised at 900°C

Conclusions

Two methods were used to characterise decarburisation of DI: direct optical observation and microhardness profiles. The correlation among the results obtained by both methods turned out to be very good.

All the specimens austenitised for more than 45 min featured surface decarburisation. The decarburised layer depth increased with increasing holding time.

Surface decarburisation was not noticed in specimens with prior ferritic matrixes and high nodule counts (NC_{900} and NC_{1800}) austenitised without protective atmosphere for less than 30 min.

The thickness of the decarburised layer diminished significantly as nodule count increased for all holding times. This is attributed to a more effective provision of carbon from the nodules towards the matrix in high nodule count parts, as a consequence of the smallest diffusion distances and the largest amount of nodule/matrix interfaces.

Within the studied range, temperature did not play a significant role on decarburised layer thickness if compared with the influence that nodule count and holding time had.

The developed equation allows accurately calculating decarburisation onset time as well as decarburised layer thickness for parts with prior ferritic matrixes and different nodule counts.

In the case of specimens with pearlitic matrixes, decarburisation is initiated at shorter times and advances in a slower manner in comparison to those with ferritic matrixes. Such difference can be ascribed to the fact that the pearlitic matrix is already saturated in carbon when the austenitisation stage is started, and therefore, it can immediately get lost.

Acknowledgement

The financial support granted by CONICET, SECYT and the National University of Mar del Plata is gratefully acknowledged.

References

1. Y.-K. Gao, X.-B. Li, Q.-X. Yang and M. Yao: *Mater. Lett.*, 2007, **61**, (2), 466–469.
2. D. Mercier, J. Lesage, X. Decoopman and D. Chicot: *NDT&E Int.*, 2006, **39**, 652–660.
3. O. N. Dogan, K. K. Schrems and J. A. Hawk: *AFS Trans.*, 2003, **111**, 949–960.
4. D. M. Stefanescu: *Mater. Sci. Eng. A*, 2005, **A413**, 322–333.
5. P. David, J. Massone and J. Sikora: *ISIJ Int.*, 2004, **44**, 1180–1187.

2

International Journal of Cast Metals Research ijc932.3d 13/4/10 14:08:02
The Charlesworth Group, Wakefield +44(0)1924 369598 - Rev 7.51n/W (Jan 20 2003)

6. P. David, J. Massone, R. Boeri and J. Sikora: *Int. J. Cast Met. Res.*, 2006, **19**, (2), 98–109.
7. V. M. Bermont and J. A. Sikora: *Int. J. Cast Met. Res.*, 1998, **11**, 51–61.
8. J. Massone, R. Boeri and J. Sikora: *Int. J. Cast Met. Res.*, 2001, **1**–**3**, 179–184.
9. D. A. Porter and K. E. Easterling: 'Phase transformations in metals and alloys', 2nd edn; 2001, Cheltenham, Nelson Thornes Ltd.

International Journal of Cast Metals Research ijc932.3d 13/4/10 14:08:07
The Charlesworth Group, Wakefield +44(0)1924 369598 - Rev 7.51n/W (Jan 20 2003)

Authors Queries

Journal: **International Journal of Cast Metals Research**
Paper: **932**
Title: **Influence of nodule count, austenitising variables and matrix on ductile iron decarburisation**

Dear Author
During the preparation of your manuscript for publication, the questions listed below have arisen. Please attend to these matters and return this form with your proof. Many thanks for your assistance

Query Reference	Query	Remarks
1	Author: Please confirm the running head.	
2	Author: Please confirm the change.	
3	Figure 2 is low quality, please supply a higher resolution version if possible.	